On-line Table 1: Image-acquisition settings ($n = 20$)

Parameter	T2	FLAIR	SWAN[a]	TIC[b]
Section orientation	Axial	Sagittal	Axial	Axial
Pulse sequence name	FSE	3D FSE	3D FGRE	3D FGRE
Time after T2 (hr:min:sec)	00:00:00	00:16:43 ± 00:03:30	00:29:16 ± 00:07:52	01:12:02 ± 00:09:45
TR (ms)	5800	7000	46	5.724–8.208
TE (ms)	76.512–80.832	123.211–131.379	23.06–23.50	1.736–2.1
TI (ms)	NA	2060–2072	NA	NA
FA	90°–125°	90°	15°	20°
FOV (cm)	19.6–23.8	23.04–25.6	20	19.2–22.4
Matrix	352 × 224	256 × 256	320 × 224	352 × 224
BW (kHz)	162.773	122.07	244.141	195.312
Voxel size (mm)	0.5469 × 0.5469 × 2	0.5 × 0.5 × 1	0.3906 × 0.3906 × 1	0.4688 × 0.4688 × 3.5 to 0.5469 × 0.5469 × 1.8[c]
Image resolution (mm) (root mean square/ Pythagorean)	1.2380/2.1443	0.7071/1.2247	0.6596/1.1424	2.0567–1.1311/3.5622–1.9591
ETL	8	140	6	1
Phase FOV (%)	70–85	100	100	80
Sampling (%)	100	100	69.1964–69.7891	100
Acquisition time (min:sec)	4:50	8:55	3:48	2:44

Note:—FGRE indicates fast gradient-recalled echo; BW, bandwidth; ETL, echo-train length; FA, flip angle.

[a] Seventeen of 20 SWAN volumes had smaller superior/inferior head coverage (68 mm) that did not include the entire brain.

[b] Obtained after 0.1 mmol/kg of either gadopentetate dimeglumine or gadobutrol (Magnevist or Gadavist, respectively) at 5 mL/s, followed by 30 mL of saline at 5 mL/s. Because 2 separate contrast doses were needed for the scanning session, the total dosage was 20 mL of Magnevist or Gadavist and 60 mL saline.

[c] Nineteen of 20 TIC image volumes had a 0.5469 × 0.5469 × 1.8 mm voxel resolution.

On-line Table 2: Fiducial landmark site location descriptions[a]

LM No.	Name of Site	Anatomic Description	X[b] (mm)	Y[b] (mm)	Z[b] (mm)
1	R. midbrain vessel	Perimesencephalic region vessel	19.93 ± 7.63	−38.06 ± 18.98	−6.15 ± 7.04
2	L. midbrain vessel	Perimesencephalic region vessel	−22.31 ± 7.06	−37.20 ± 16.61	−7.88 ± 6.27
3	R. MCA bifurcation	MCA bifurcation	33.89 ± 5.29	6.06 ± 5.62	−9.37 ± 7.08
4	L. MCA bifurcation	MCA bifurcation	−36.05 ± 6.66	4.06 ± 7.30	−8.92 ± 7.87
5	R. TSV-septal junction region	Venous angle	1.00 ± 2.40	−11.26 ± 5.99	13.42 ± 5.46
6	L. TSV-septal junction region	Venous angle	−2.50 ± 2.32	−10.45 ± 3.92	12.94 ± 5.58
7	Vein of Galen	Top of straight sinus	−4.29 ± 6.52	−49.56 ± 7.46	13.49 ± 6.59
8	R. posterior midlevel	Posterior Sylvian vessel	43.76 ± 8.85	−37.18 ± 18.62	16.13 ± 7.22
9	R. anterior midlevel	Anterior Sylvian vessel	36.53 ± 5.21	18.24 ± 7.65	11.84 ± 8.78
10	L. posterior midlevel	Posterior Sylvian vessel	−43.01 ± 7.75	−32.08 ± 13.17	18.40 ± 7.42
11	L. anterior midlevel	Anterior Sylvian vessel	−36.49 ± 6.03	15.81 ± 10.62	9.57 ± 7.81
12	Superior midline	Superior interhemispheric sulci region vessel	−1.53 ± 9.08	−15.01 ± 27.62	37.80 ± 8.53
13	Far anterior	Anterior, midaxial region vessel	−0.87 ± 6.77	50.97 ± 10.52	8.88 ± 10.12
14	Posterior/inferior	Torcular region inflow vessel	−4.49 ± 11.15	−84.67 ± 8.92	−14.71 ± 4.93
15	Falx cerebri region	Superior sagittal sinus region inflow vessel	−0.53 ± 4.87	−14.62 ± 18.52	68.57 ± 7.10

Note:—L. indicates left; R., right; TSV, trans-septal vein.

[a] Refer to Fig 1 for graphic descriptions.

[b] Right Anterior Superior (RAS) coordinate system (positive axes to R, A, and S) with the anterior commissure as the origin, based on the International Consortium for Brain Mapping 152 Nonlinear Symmetric 2009b template of the Montreal Neurological Institute (http://www.bic.mni.mcgill.ca/ServicesAtlases/ICBM152NLin2009; $n = 20$ for each landmark).

On-line Table 3: Target-to-registration error and Euclidean effectiveness ratio values for each registration and sequence ($n = 20$)[a]

Registration Experiment	FLAIR		SWAN		T1C	
	TRE (mm)	EER	TRE (mm)	EER	TRE (mm)	EER
Pre	2.07 ± 0.55	1.000	2.63 ± 0.62	1.000	3.65 ± 2.00	1.000
GE	1.74 ± 0.33	0.672	1.46 ± 0.26[b]	0.259	1.06 ± 0.16[c,f]	0.096[f]
Rigid CC	1.62 ± 0.42[b]	0.556	1.75 ± 0.67[b]	0.440	2.39 ± 1.98	0.560
Rigid MI	1.55 ± 0.46[b,f]	0.493[f]	1.55 ± 0.39[d]	0.313	1.95 ± 1.15	0.406
Affine CC	1.72 ± 0.46	0.653	1.57 ± 0.43[b]	0.323	1.27 ± 0.35[b]	0.170
Affine MI	1.82 ± 0.62	0.757	1.34 ± 0.23[c,f]	0.181[f]	1.07 ± 0.14[e]	0.100
Rigid LM	1.15 ± 0.26[c]	0.107	1.17 ± 0.24[c]	0.068	0.86 ± 0.13[c]	0.025
Affine LM	1.04 ± 0.24[c]	0.000	1.06 ± 0.26[c]	0.000	0.79 ± 0.14[c]	0.000

Note:—Pre indicates preregistration. FLAIR: Dunnett test; SWAN, T1C: Dunn test.

[a] Footnotes b–e indicate statistically significant TRE differences from preregistration values.

[b] $P \leq .05$.

[c] $P \leq .0001$.

[d] $P \leq .01$.

[e] $P \leq .001$.

[f] The best-performing registration for that sequence and metric.

On-line Table 4: Statistical effectiveness ratio values for each registration and sequence, using patient-averaged data ($n = 20$)

Registration Experiment	FLAIR	SWAN	T1C
Pre	1.000	1.000	1.000
GE	0.980	0.475	0.929
Rigid CC	0.693	0.412	0.565[a]
Rigid MI	0.573[a]	0.450	0.704
Affine CC	0.758	0.435	0.903
Affine MI	0.680	0.352[a]	1.007
Rigid LM	0.183	0.130	0.260
Affine LM	0.000	0.000	0.000

[a] Best-performing registration for that sequence.

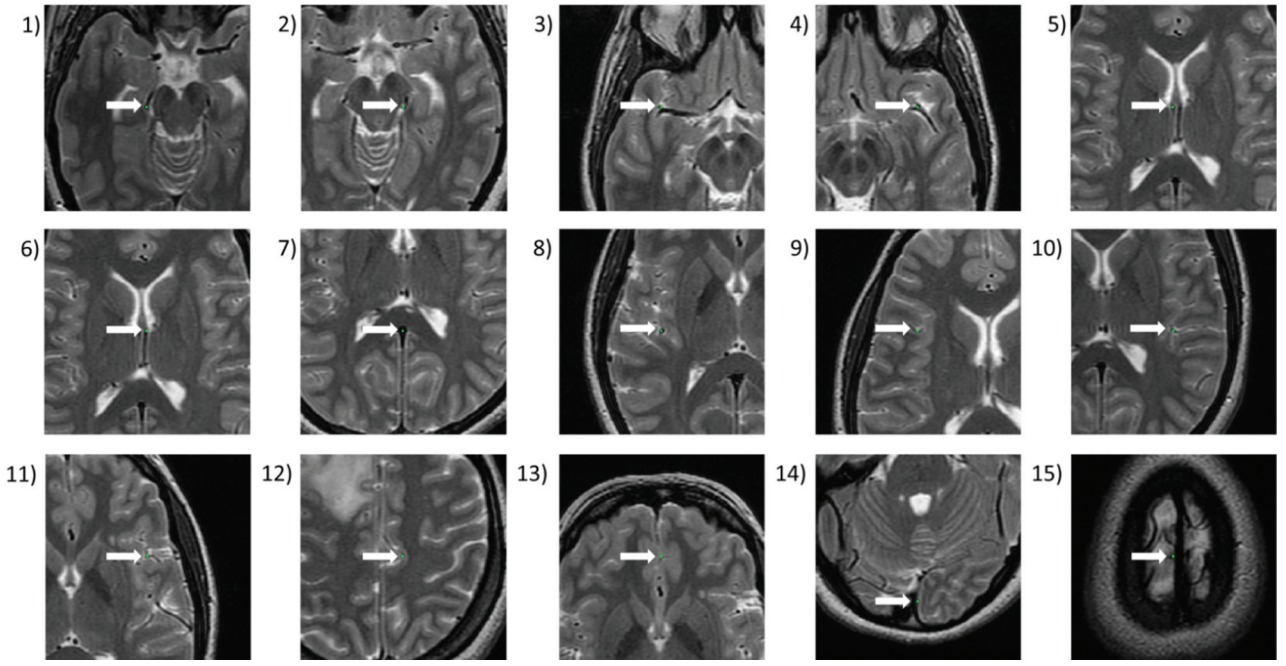

ON-LINE FIG 1. Axial T2-weighted views of fiducial landmark locations in a single patient, indicated by *green dots* with *white arrows*.

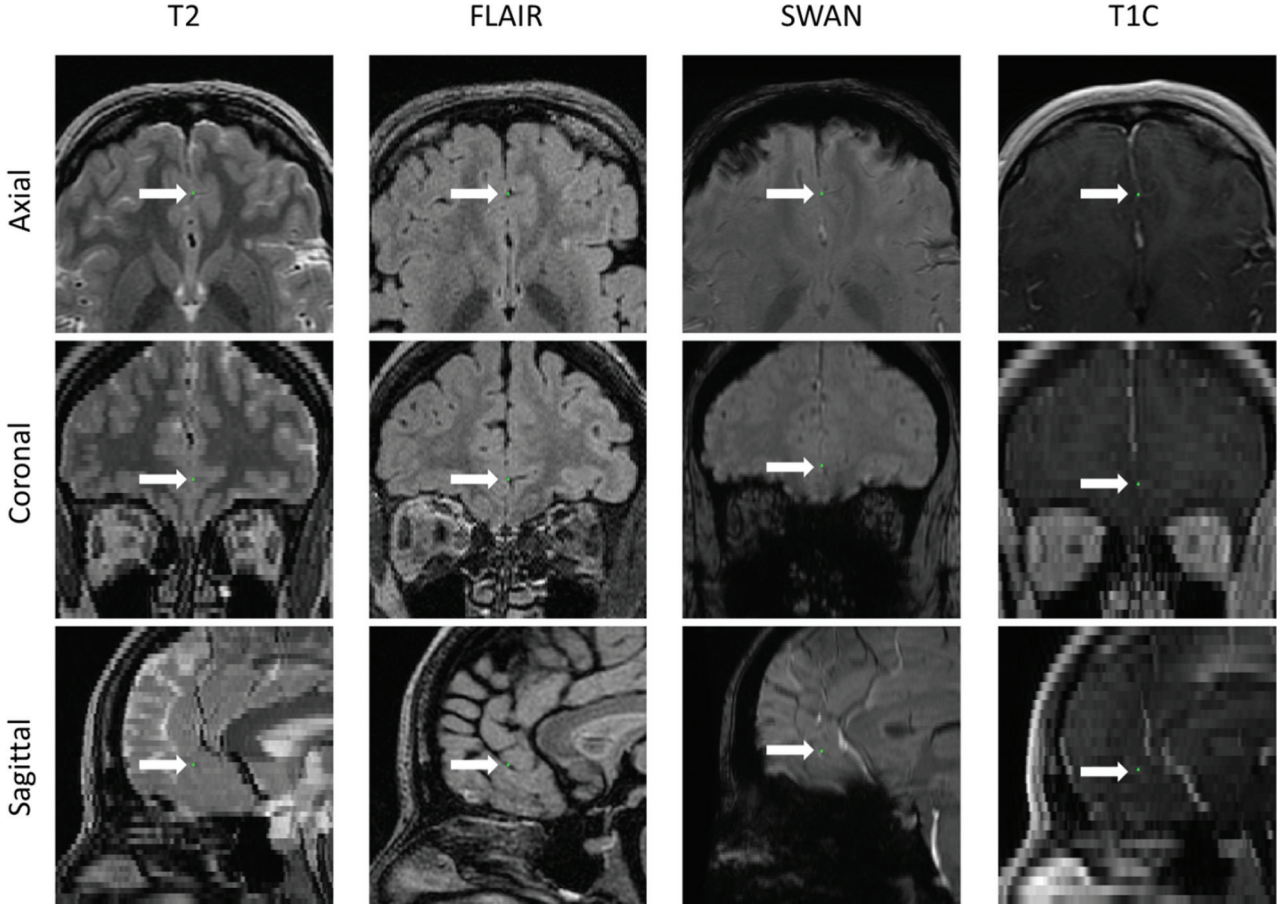

ON-LINE FIG 2. Fiducial landmark site 13 in 3-plane views for T2, FLAIR, SWAN, and T1C sequences, indicated by *green dots* with *white arrows*.

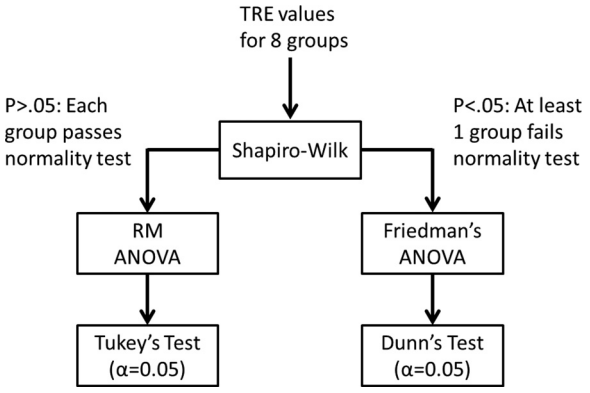

ON-LINE FIG 3. Statistical testing flowchart for target-to-registration error results for a single sequence. RM ANOVA indicates repeated measures ANOVA.

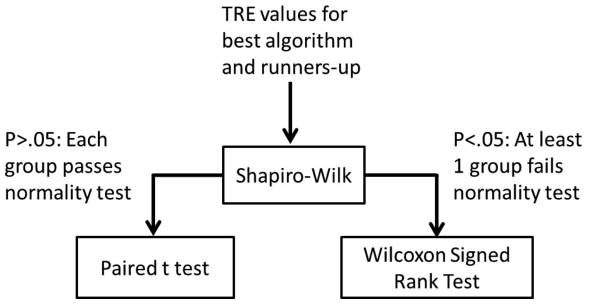

ON-LINE FIG 4. Statistical testing flowchart for TRE pair-wise comparisons of a sequence's best-performing algorithm and its runners-up.

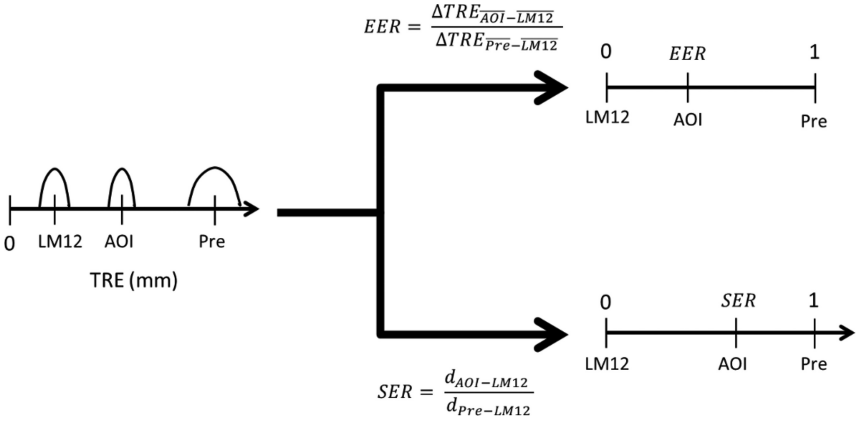

ON-LINE FIG 5. Conversion of target-to-registration error to the Euclidean effectiveness ratio and statistical effectiveness ratio for an AOI. LM12 indicates affine LM registration; Pre, pre-registration.

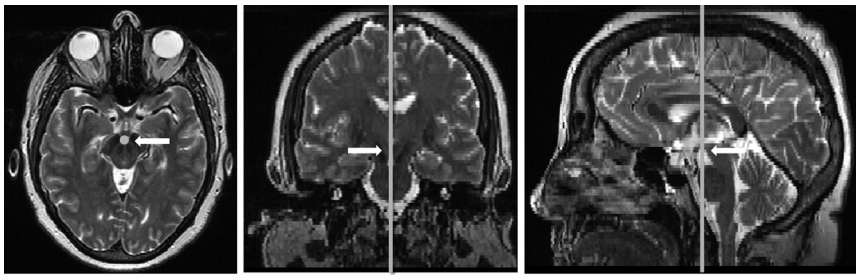

ON-LINE FIG 6. User-defined fulcrum point (*white arrows*) along a rotational axis in line with the dens. TRE behavior was analyzed on the basis of the Euclidean distance from this point.

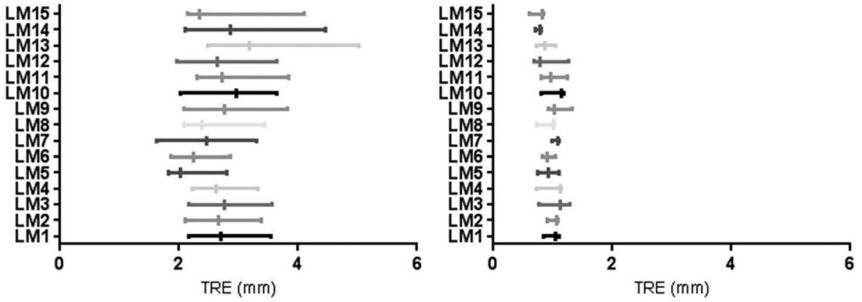

ON-LINE FIG 7. Baseline (*left*) and affine LM (*right*) TRE values for different landmark sites, averaged for FLAIR, SWAN, and T1C ($n = 20$).

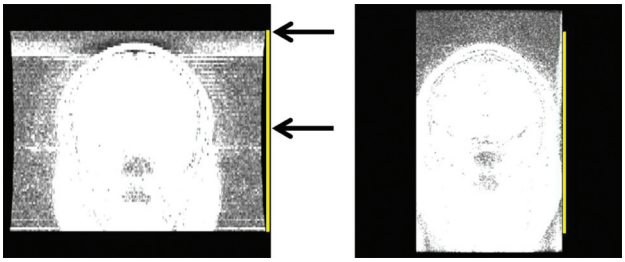

ON-LINE FIG 8. Coronal views of a native axial T2 sequence (*left*) and a native sagittal FLAIR sequence (*right*). Intensity windows have been leveled to make the acquisition edges visible. Left/right distortion correction has been applied to the left T2 image (note the side curvature that flares out at the top and bottom) but not the right FLAIR image. The lack of such correction makes anatomy on the FLAIR images appear smaller along the left/right axis, especially closer to the superior/inferior edges of the image volume, away from the isocenter where the magnetic gradients are weaker.